2,3,6-Tricarboxylate Cellulose as a Fully Biodegradable Flocculant: Efficient Synthesis and Flocculation Performance

Kexin Chen,[a] Weijun Lv,[b,*] Wei Chen,[a] Yifeng Wang,[c] Yong Zhang,[a,*] Xiumei Zhang,[a] and Juming Yao [a]

Cellulose-based flocculants have shown excellent performance for wastewater flocculation, being low-cost and eco-friendly. However, they are still disturbed by the problems of incomplete biodegradability and unstable chemical structure. In the present study, 2,3,6-tricarboxylate cellulose (TCC) was developed as a novel fully biodegradable flocculant to deal with the preceding problems. The key carboxymethylation of cellulose was first carried out to make the subsequent $NaIO_4$ oxidation occur under homogeneous conditions, which greatly enhanced the carboxylate content of the final TCC products. The chemical structure and solution properties of the TCCs were characterized by Fourier transform infrared spectroscopy (FTIR), X-ray diffractometer system (XRD), field emission scanning electron microscopy (FESEM), charge density, particle size, and zeta potential. The flocculation performance of the TCCs was evaluated preliminarily by the turbidity removal of kaolin suspension. The positive results showed that all the TCC products had high carboxylate contents (more than 10 mmol/g) and zeta potentials. They exhibited excellent flocculation performance for the kaolin suspensions, in which the residual turbidities decreased from 610 to 14.9 NTU. Considering the degradation of cellulose caused by excessive $NaIO_4$ oxidation, the TCC IV, together with its synthesis technology, could be used for practical applications in wastewater flocculation.

Keywords: Tricarboxylate cellulose; Natural flocculant; Homogeneous oxidation; Carboxylate content; Full-biodegradation

Contact information: a: The Key Laboratory of Advanced Textile Materials and Manufacturing Technology of the Ministry of Education, College of Materials and Textiles, Zhejiang Sci-Tech University, Hangzhou 310018, China; b: The National Engineering Laboratory for Pulp and Paper Technology, China National Pulp and Paper Research Institute, Beijing 100020, China; c: The Hydrology and Water Resources Monitoring Station in Hangzhou, Hangzhou 310016, China;
** Corresponding author: zhangyong@zstu.edu.cn, lvweijun761005@163.com*

INTRODUCTION

Wastewater, generated from various industries and containing toxic chemical contaminations, is discharged into natural water bodies and can cause serious environmental and ecological problems. Flocculation is an economical and effective technique for removal of particle contaminants, such as organic pollutants in chemical and papermaking wastewater (Faust *et al*. 2014), as well as dyes from dyeing effluent (Yang *et al*. 2013a). In recent years, synthetic organic polymer flocculants, especially polyacrylamide and poly diallyl dimethyl ammonium chloride, have seen extensive application because of their mature production technology and high flocculation efficiency.

However, their poor degradability and hazardous degradation products eventually remain a potential threat to the natural environment and human health (Faris *et al*. 2015).

Natural polymer-based flocculants, because of their non-toxicity, biodegradability, and regeneration, can meet the increasing demand for eco-friendly and sustainable materials. Recently, they have become a key research focus around the world, *e.g.*, starch-based flocculants (Yang *et al*. 2014), inulin-based flocculants (Rahul *et al*. 2014), and cellulose-based flocculants (Vandamme *et al*. 2015). Among these natural materials, cellulose is the most abundant natural polymer worldwide and can be used as a raw material to develop various eco-friendly materials (Kureli and Doganay 2015). Based on its physical properties and chemical reactivity, cellulose is a suitable alternative for modification and preparation of natural flocculants. In current cellulose-based flocculants, semi-natural flocculants that graft copolymers onto a cellulose backbone have been an important and often-used type of flocculant (Zhu *et al*. 2015). However, these flocculants have the same environmental problems as synthetic flocculants because of their incomplete biodegradability and unstable chemical structure.

To solve this problem, it is a good way to obtain fully biodegradable flocculants by modifying cellulose directly. One of the core technologies is the introduction of carboxyl groups onto cellulose macromolecules to increase their charge density, such as preparations of dicarboxylic acid nanocellulose (Suopajärvi *et al*. 2013), carboxymethyl cellulose (Qi *et al*. 2010), and dicarboxyl cellulose (Zhu *et al*. 2015). The resultant flocculants are completely biodegradable and do not provide non-secondary contamination to the environment. However, the biggest challenge in this process now is the limited carboxylate content, which leads to lower charge density on the flocculants. This results in a large impact on their flocculation performance. In previous work, C6-carboxyl cellulose was synthesized by 2,2,6,6-tetramethylpiperidine-1-oxyl (TEMPO)-mediated oxidation, and its carboxylate content was 1.69 mmol/g (Okita *et al*. 2010). To further develop this work, Takaichi and Isogai (2013) adopted the 2-azaadamantane N-oxyl (AZADO) /NaBr/NaOCl system to oxidize softwood pulp for the production of tricarboxylate cellulose. The carboxylate content of this product grew to 9.70 mmol/g, which was contributed by the three carboxyl groups grafted on the cellulose skeleton (Takaichi *et al*. 2014). However, the reagents used in this process are expensive, substantially increasing production costs. In Qi's work, carboxylmethylation of cellulose was investigated to obtain carboxymethyl cellulose with a carboxylate content of 1.48 mmol/g (Qi *et al*. 2010). Although the carboxyl groups were conveniently and mildly formed in this method, the final carboxylate content was still relatively low.

Another method for carboxyl cellulose preparation is $NaIO_4$ oxidation followed by $NaClO_2$ oxidation. The C2 and C3 of anhydroglucose units (AGUs) are first oxidized to aldehyde groups through $NaIO_4$ oxidation; they are then continuously oxidized to carboxyl groups by $NaClO_2$. Liimatainen *et al*. (2012) adopted this process to synthesize dicarboxyl cellulose (DCC) with a carboxylate content of 1.75 mmol/g. The aldehyde content of its precursor (dialdehyde cellulose, DAC) was 1.68 mmol/g. The work of Kim and Kuga (2001) also resulted in a similar carboxylate content of 0.92 mmol/g in DCC and aldehyde content of 0.93 mmol/g in DAC. In our most recent work, a one-step homogeneous process was developed to synthesize DCC. The aldehyde and carboxylate contents were also both in the range of 2 to 3 mmol/g (Zhu *et al*. 2015). The low aldehyde content severely restricts the formation of carboxyl groups on cellulose macromolecules. A breakthrough in the oxidation process is strongly desired.

Recently, it was found by the authors that conducting carboxymethylation first on cellulose, followed by $NaIO_4$ oxidation, can enhance the aldehyde content of the resultant DAC. To obtain evidence for this, a novel $NaIO_4$ and $NaClO_2$ oxidation route was investigated to synthesize a 2,3,6-tricarboxylate cellulose (TCC) with high carboxylate content in a cost-effective manner, designed to result in fully biodegradable cellulose flocculants based on the biodegradability of cellulose (Klemm *et al.* 2005; Liu *et al*. 2008). The chemical structure of the TCC product was characterized by Fourier transform infrared spectroscopy (FTIR), X-ray diffractometer system (XRD), and field emission scanning electron microscopy (FESEM). The charge density (CD), aldehyde and carboxylate contents, particle size, and zeta potential of the TCC were also analyzed in detail. Meanwhile, a standard kaolin suspension was employed to evaluate the flocculation performance of the TCCs.

EXPERIMENTAL

Materials

α-Cellulose powder (DP 170-200, size 25 μm; Aladdin Chemistry Co. Ltd., China) and kaolin particles (superfine size of 11 μm; Aladdin Chemistry Co. Ltd., China) were used as received. The reagents for dissolution (NaOH, H_2NCONH_2), oxidation ($NaIO_4$, $NaClO_2$, $COHCH_2CH_2OH$), carboxyl and aldehyde content analysis ($NH_2OH.HCl$, NaCl, CH_3COOH, $CH_3COONa.3H_2O$), poly (dimethyldiallylammonium chloride),and auxiliary process ($AlCl_3.6H_2O$, CH_3CH_2OH) were of analytical grade (Guoyao Chemcial Reagent Co., Ltd., China), and used without further purification. Commercial-grade carboxymethyl cellulose (CMC) and anionic polyacrylamides (APAMs) with the molecular weight of 90 thousand and 12 million were supplied by the Aladdin Chemistry Co. Ltd., China. Deionized water, produced by a Millipore Direct-Q 5 ultrapure water system (EDM Millipore Co., Germany), was used throughout the experiments.

Synthesis of TCC

Carboxymethylation of cellulose

Anionic cellulose (AC) was synthesized through carboxymethylation of cellulose. One gram of α-cellulose powder and 50 mL of urea-NaOH aqueous solution (12 wt% urea and 7 wt% NaOH, precooled at 4 °C) were added to a 250-mL flask. The mixture was stirred vigorously to make it well dispersed. Then the suspension was cooled to -12 °C for at least 1.5 h to obtain a transparent and viscous cellulose solution (Yang *et al*. 2013a). Next, 4.3 g of sodium monochloroacetate was added to the cellulose solution and vigorously stirred by a magnetic stirrer in a water bath at 55 °C (Qi *et al*. 2010). After 5 h, the mixture was neutralized with 3 M HCl and extracted by 95% ethanol. After centrifugation, the AC product was dried in a freeze-dryer.

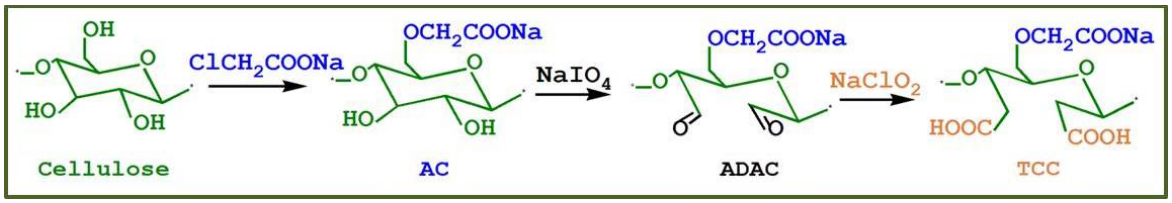

Fig. 1. Proposed synthesis route for the TCC product (cellulose: α-cellulose powder, AC: anionic cellulose, ADAC: anionic dialdehyde cellulose, TCC: 2,3,6-tricarboxylate cellulose)

$NaIO_4$ and $NaClO_2$ oxidations of AC

Anionic dicarboxyl cellulose (ADAC) with various charge densities was synthesized by first oxidizing the hydroxyl groups on C2 and C3 of AGUs of the AC using $NaIO_4$. The aldehyde groups on the obtained ADAC were subsequently oxidized to carboxyl groups by $NaClO_2$ to produce TCC. In brief, 1 g of AC was subjected to oxidation with 0.8 to 2.4 g $NaIO_4$ at 50 °C in the dark for 3 h (Liimatainen *et al*. 2012). The residual $NaIO_4$ was neutralized with excess ethylene glycol. The product was subsequently extracted by 500 mL of ethanol, centrifuged, washed, and further oxidized with $NaClO_2$ in an acetic acid buffer (pH 4.5) for 48 h at room temperature to obtain the TCC. The resultant TCC product was finally extracted and washed by ethanol and water, respectively. The proposed synthesis route of the TCC is depicted in Fig. 1.

Characterization of AC, ADAC, and TCC

Analysis of aldehyde and carboxylate contents

The aldehyde content of ADAC was determined by an oxime reaction as described in the literature (Sirvio *et al*. 2011). The ADAC was converted to oxime by Schiff's base reaction using $NH_2H_2O.HCl$. First, 0.1 g of ADAC was suspended in 30 mL of deionized water and the pH was adjusted to 4.5 with 0.1 M HCl or NaOH. The ADAC suspension was added to the $NH_2H_2O.HCl$ solution (0.43 g in 20 mL H_2O, pH 4.5). The mixture was stirred for 24 h at room temperature. Then, the released HCl was titrated using 0.01 M NaOH. The aldehyde content of the ADAC was calculated through the consumption of the 0.01 M NaOH. The carboxylate contents of AC and TCC were analyzed with a DDS-307 conductivity meter (Shanghai REX Instrument Factory, China) using the procedure described by Zhu *et al*. (2015). Briefly, 0.3 g of dried sample was added to a solution consisting of 5 mL of 0.01 M NaCl and 55 mL of H_2O. The mixture was sufficiently stirred to obtain a well-dispersed slurry. Then, 0.1 M HCl was added to the slurry to control its pH in the range of 2.5 to 3.0. The slurry was titrated with 0.04 M NaOH at a rate of 0.1 mL/min to pH 12. The carboxylate content was determined based on the conductivity and pH curves.

Characterization of products

The zeta potential and particle size of the AC and TCC were investigated using a Malvern Nano ZS90 (Malvern Instruments Ltd., USA). The solution for zeta potential measurement was at neutral pH in 0.5 mM [Na^+] buffer. The charge densities of the AC and TCC solutions (1 wt%) were tested by polyelectrolyte titration with a cationic polyelectrolyte (poly- dimethyldiallylammonium chloride, PDADMAC, 0.0001 M) using a Mütek PCD 03 particle charge detector (BTG Co., Sweden). The FTIR spectra of the cellulose, AC, ADAC, and TCC were recorded using a Thermo Nicolet 5700 FTIR spectrometer (Thermo Fisher Scientific Inc., USA). The crystallinity of the cellulose, AC, ADAC, and TCC (powder samples) was measured by Bruker AXS D8 (Bruker Co., Germany) X-ray diffractometry. The crystallinity index (CI) of samples was calculated through peak fitting and calculating program (Java and UML Developers' Environment). The morphology of samples was photographed using a Hitachi S4800 FESEM (Hitachi Ltd., Japan).

Evaluation of TCC Coagulation-Flocculation

The flocculation of the TCC products was evaluated by measuring the residual turbidity of kaolin suspension with a concentration of 1 g/L after coagulation-flocculation.

The initial pH of the kaolin suspension was 6. The experiments were carried out by adding Al^{3+} (150 mg/L, optimized dosage, derived from $AlCl_3.6H_2O$) as coagulant into 100 mL of kaolin suspension. The mixture was stirred at 200 rpm for 1 min. Then, a set amount of TCC was added with slow stirring at 40 rpm for 3 min. Finally, the suspension was allowed to settle for 10 min and the residual turbidity of the supernatant was measured by Turb 550 turbidity (Wissenschaftlich-Technische Werkstätten GmbH., Germany). The zeta potential of the initial and coagulated kaolin suspension was monitored to assess the influence of pH in the coagulation process. The range of pH in the kaolin suspension increased from 3 to 10, as adjusted by 0.1 M HCl or NaOH solution.

RESULTS AND DISCUSSION

Optimization of ADAC Synthesis

Because of the high crystallinity of natural cellulose, a large amount of $NaIO_4$ and a long oxidation time are required to obtain high aldehyde content in DAC. In the present work, a novel synthesis route was designed to solve this problem. Water-soluble AC was prepared before $NaIO_4$ oxidation to reduce the crystallinity of cellulose. Since the excellent water-solubility of AC, efficient $NaIO_4$ oxidation could be carried out under homogeneous conditions to obtain the target ADACs with high aldehyde content. Meanwhile, considering the relatively high cost of $NaIO_4$, a single-factor experiment was conducted to explore an economical and eco-friendly oxidation process. The detailed experimental schedule is presented in Table 1.

Table 1. Optimization of $NaIO_4$ Dosage for ADAC Synthesis

Samples	$NaIO_4$ to AC (mass ratio)	Reaction temperature (°C)	Reaction time (h)	Aldehyde content (mmol/g)
ADAC I	1.0	50	3	8.70
ADAC II	1.5	50	3	11.60
ADAC III	2.0	50	3	13.00
ADAC IV	2.5	50	3	13.30
ADAC V	3.0	50	3	13.55

The aldehyde contents of the resultant ADAC (I through V) increased with increasing mass ratio of $NaIO_4$ to AC, especially for ADAC I through III. Furthermore, the aldehyde contents of ADAC III-V all exceeded the theoretical maximum value of 12.34 mmol/g. This was attributed to the fact that in addition to the almost complete transformation of the hydroxyl groups on C2 and C3 of the AC, the residual hydroxyl groups on C6 were also oxidized to aldehyde groups by $NaIO_4$ (Sirviö *et al*. 2011). As a result, relatively high aldehyde contents of 8.70 to 13.55 mmol/g and low consumption of $NaIO_4$ for ADAC synthesis were achieved in comparison with other works.

Synthesis of TCC

The next transformation from aldehyde group to carboxyl group was conducted by chlorite oxidation to obtain TCC flocculants with high negative zeta potential and charge density. The precursor ADAC I-V were transferred into acetic acid buffer and subsequently oxidized by $NaClO_2$ for 48 h to synthesized the corresponding TCC I-V. Table 2 exhibits the electrochemical characteristics of the TCC products with various oxidation degrees.

The maximum carboxylate content was determined to be 14.63 mmol/g of TCC V, which was lower than the theoretical maximum value of 18.52 mmol/g. This value also indicated that the aldehyde groups on ADAC were almost completely transformed to the carboxyl groups of TCC. This fact confirmed that the high carboxylate content was closely related to the oxidation degree of ADAC and the $NaIO_4$ oxidation was remarkably efficient under homogeneous conditions. Correspondingly, the zeta potentials of the TCCs increased from -23.3 to -41.8 mV with increasing carboxylate content. The CDs of the TCCs and AC presented high consistency with their carboxylate contents. Moreover, the variation of particle size from AC to TCC indicated that the degradation of cellulose macromolecules occurred during the $NaIO_4$ and $NaClO_2$ oxidation processes. This might affect the performance when the TCC is employed as a flocculant.

Table 2. Carboxylate Content, Particle Size, Charge Density, and Zeta Potential in 0.5 M [NaCl] Buffer of TCC Products from ADACs with Various Oxidation Degrees

Samples	Carboxylate content (mmol/g)	Particle size (nm)	Charge density (mmol/g)	Zeta-potential (mV)±σ
AC	1.150±0.01	15324±351	0.9800±0.10	-15.4±2.5
TCC I	10.36±0.02	3760.0±113	10.33±0.05	-23.3±2.4
TCC II	12.71±0.08	1656.0±105	12.73±0.04	-29.6±2.8
TCC III	13.93±0.05	875.10±61	13.91±0.08	-30.1±2.1
TCC IV	14.46±0.07	615.40±46	14.43±0.03	-35.6±1.4
TCC V	14.66±0.09	442.80±53	14.67±0.07	-41.8±2.6

Characterization of AC, ADAC, and TCC

Chemical structure

The structural changes of the cellulose and related products were characterized by FTIR. Figure 2 presents the FTIR spectra of the cellulose, AC, ADAC, and TCC. The absorption peak of the AC at 1603 cm^{-1} indicated that COO^- was successfully introduced onto the cellulose skeleton.

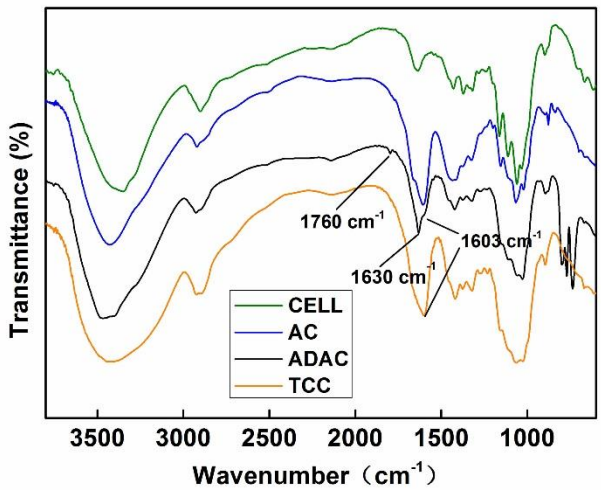

Fig. 2. FTIR spectra of the cellulose, AC, ADAC, and TCC

The spectra for the ADAC showed characteristic bands at 1760 and 893 cm^{-1}. They were assigned to carbonyl groups and hemiacetals (Teotia 2012). It was further observed

that the band at 1603 cm^{-1} moved to 1630 cm^{-1}. This was attributed to the formation of aldehyde groups. According to the spectrum of the TCC, the disappearance of aldehyde bands at 1760 cm^{-1} and generation of an intense carboxyl characteristic peak at 1603 cm^{-1} demonstrated the important transformation from aldehyde group to carboxyl group on the TCC macromolecules, confirming that the target TCC product was successfully synthesized.

Crystallinity

The influences of carboxymethylation and oxidation on the crystal structure of cellulose are presented in Fig. 3. As shown in Fig. 3a, AC had a crystallinity of 36.4%, which was much lower than that of the original cellulose, at 68.4%. This suggests that the crystalline region of cellulose was damaged extensively by the carboxymethylation of the hydroxyl groups on C6. Meanwhile, the typical peak of cellulose at 22.6° disappeared and a broadened peak at 21.7° was generated with the formation of the crystalline structure on the AC. In Fig. 3b, in the X-ray diffraction pattern of ADAC, disordered amorphous regions were observed. The well-defined AC pattern was obviously diminished during the oxidation. The calculated crystalline index of the ADAC sharply decreased to 17.1%, mostly caused by the ring-opening reaction of AGUs, changes in hydrogen bonding, and degradation of cellulose chains (Teotia 2012). With the subsequent transformation from ADAC to TCC, the crystalline region near 21° was re-established by the formation of new hydrogen bonds from the carboxylate groups of TCC. The CI of the TCC finally returned to 49.8%. The specific crystallinity index, particle Size and L/D of the series products are summarized in Table 3.

Table 3. Crystallinity index, Particle Size, and L/D of the series products

Sample	Crystallinity index (%)	Particle size (nm)	L/D
Cellulose	68.4	82834±236	3.42
AC	36.4	15324±351	6.21
ADAC	17.1	937.50±127	16.3
TCC	49.8	615.40±46.0	63.5

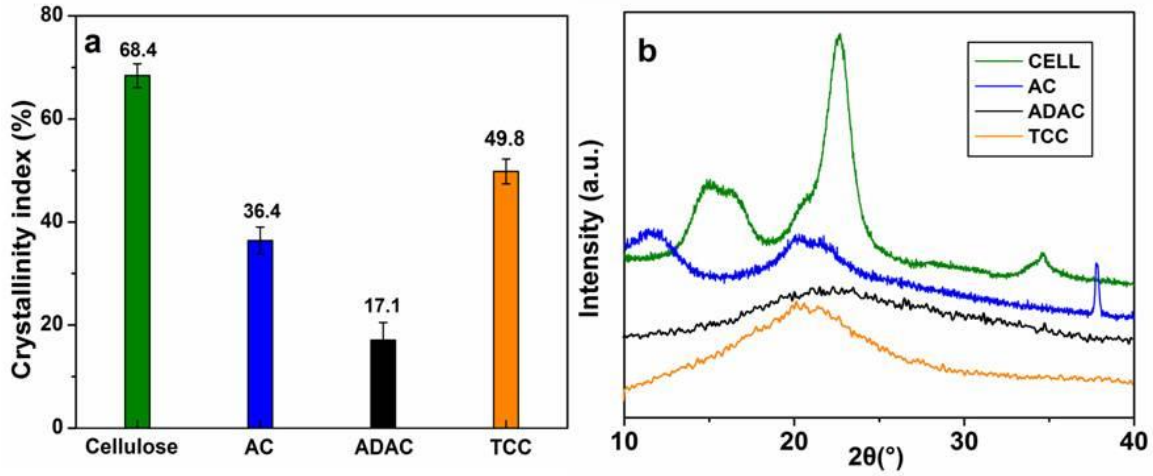

Fig. 3. Transformation of crystal structure of cellulose, AC, ADAC, and TCC: (a) crystallinity index, (b) XRD pattern

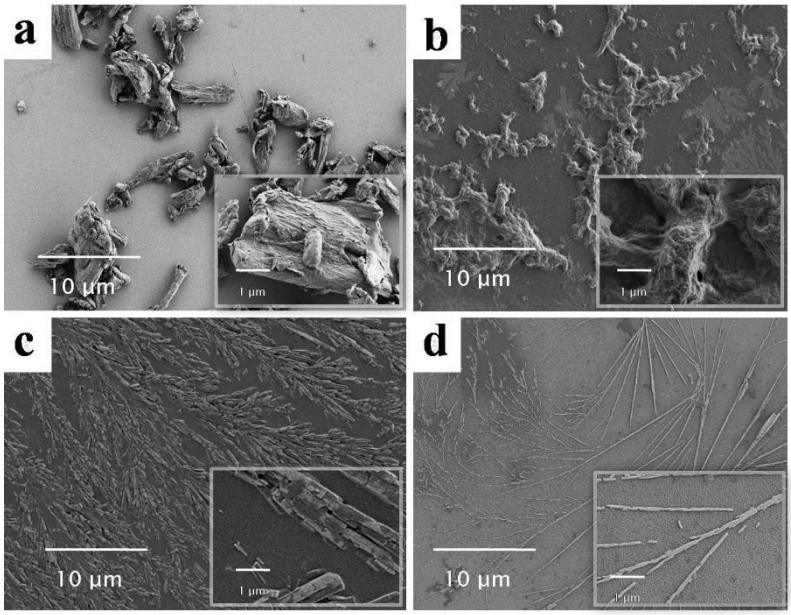

Fig. 4. FESEM pictures of (a) original cellulose, (b) AC, (c) ADAC, and (d) TCC

Morphology

Figure 4 exhibits the surface morphologies of cellulose, AC, ADAC, and TCC. It can be seen from Fig. 4a that the surface of the original cellulose was rough and wrinkled with the form of rod-like fibers. As shown in Fig. 4b, the surface of the AC became amorphous and showed a disordered distribution after carboxymethylation. This was primarily due to the destruction of crystalline regions on cellulose, which provided the lower degree of crystallinity and better water-solubility to the AC. In the case of oxidized cellulose, Fig. 4c shows that the morphology and structure of the ADAC was reshaped. The L/D (length-diameter) ratio also became higher than that of the AC. With the following conversion from ADAC to TCC, shown in Fig. 4d, the *L*/*D* ratio of the TCC was further increased, which was attributed to the destruction of intermolecular H-bonding on cellulose macromolecules. Moreover, the distribution of the TCC in Fig. 4d was very regular. This is mostly caused by electrostatic repulsions from the newly formed carboxyl groups of the TCC product.

Coagulation-Flocculation of Kaolin Suspension

Optimization of coagulant dosage

To destabilize a kaolin suspension, the process of coagulation is necessary and the dosage of coagulant is a crucial factor in coagulation. Inorganic Al^{3+} was employed as a coagulant in the subsequent coagulation-flocculation of the kaolin suspension. Figure 5 shows the residual turbidity and zeta potential variations of the kaolin suspension (1 g/L, original turbidity 610 NTU) with increasing coagulant dosage at the initial pH 6. The Al^{3+} solution ($AlCl_3.6H_2O$, 10 g/L) was used during the coagulation process. The residual turbidity of the kaolin suspension decreased substantially before the Al^{3+} dosage of 150 mg/L. Then, the turbidity decline was mild with increasing Al^{3+} dosage. The residual turbidity reached the lowest point, 90.5 NTU, when the Al^{3+} dosage was 400 mg/L. Simultaneously, the zeta potential of the kaolin suspension was close to zero at this point. This phenomenon indicated that the charge neutralization mechanism played a major role

in this coagulation process (Yang *et al*. 2013b). Considering the low cost of practical application, the optimal Al^{3+} dosage of 150 mg/L was adopted for subsequent TCC flocculation.

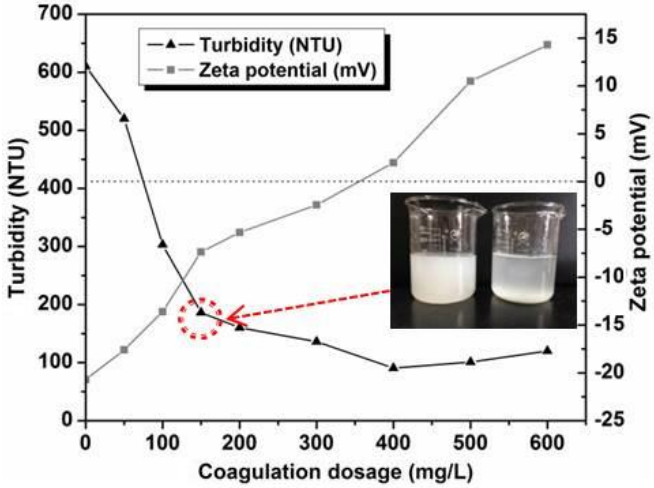

Fig. 5. Residual turbidity of the kaolin suspension (1 g/L) as a function of coagulant dosage (Al^{3+}) after the coagulation (pH of the kaolin suspension as 7 and settling time as 30 min).

Influence of pH on coagulation

Coagulation with Al^{3+} was tested as a function of pH to obtain the feasible pH conditions and help to explain its assistant role in the subsequent TCC flocculation. Figure 6a indicates that the coagulation showed better performance in acidic conditions. After the point of pH 6, the residual turbidity of kaolin suspension remained approximately constant with increasing pH. This can be explained by the reaction between Al^{3+} and OH^- in the suspension. With increasing pH, Al^{3+} combined with OH^- to form AlO^{2-}, which maintained the pH stability of the suspension (Wei *et al*. 2015). This was also confirmed in Fig. 6b, in which the final pH reached a plateau after coagulation in the initial pH range from 5 to 10. In Fig. 6c, because of its negative zeta potential, kaolin served as an anionic particle in the suspension.

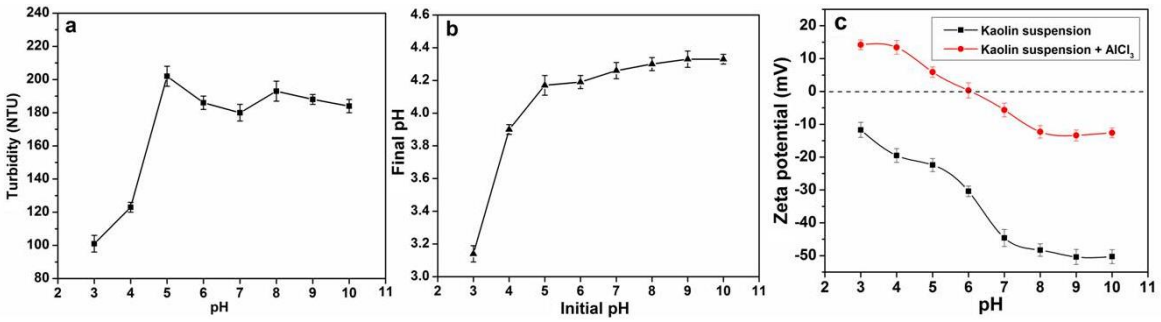

Fig. 6. pH influence of Al^{3+} coagulation on the kaolin suspension (1 g/L): (a) coagulation performance of Al^{3+} at various pH values, (b) pH variation after Al^{3+} coagulation, (c) zeta potential of the kaolin suspension with and without Al^{3+} in the pH range from 3 to 10

After the introduction of Al^{3+}, the zeta potential of the suspension was positive when the pH was lower than 6, which was partly caused by the formation of amorphous Al^{3+} hydroxide ($Al(OH)^{2+}$ or $Al(OH)_2^+$). This could be illustrated by the synergistic effect of charge neutralization and sweeping during the coagulation process. With increasing pH, the zeta potential of the suspension became negative, which revealed that this coagulation

was primarily based on the charge neutralization mechanism (Li *et al*. 2006). Considering the economic and mild operation, an initial pH 6 for the kaolin suspension was chosen for subsequent TCC flocculation.

Influence of TCC dosage on coagulation-flocculation

The dosage of flocculant is an important parameter for coagulation-flocculation. Excess or insufficient flocculant will both cause an increase in the residual turbidity of the effluent. Figure 7a presents the flocculation performance of the TTC products with respect to the kaolin suspension (1 g/L, original turbidity 610 NTU) with the assistance of Al^{3+}. The residual turbidities of the kaolin suspensions after the coagulation-flocculation by Al^{3+} and TCCs declined sharply with increasing dosage of TCC before 80 mg/L, and then changed slightly. All the synthesized TCCs exhibited excellent flocculation performance for the kaolin suspensions, in which the residual turbidities declined from 610 to a range of 69.4 to 14.9 NTU. The corresponding turbidity removal ratios reached 88.6% to 97.6%, respectively. In comparison with the single coagulation of Al^{3+} shown in Fig. 5, the combined coagulation-flocculation with Al^{3+} and TCCs achieved a better performance with lower residual turbidity and smaller coagulant dosage. Considering flocculation efficiency and economy, a TCC dosage of 80 mg/L was adopted for the following flocculation experiments.

In addition, the flocculation of TCCs I through IV was obviously strengthened with an increase in carboxylate content in TCC. TCC IV achieved the best flocculation performance (residual turbidity declined to 14.9 NTU). However, in the case of TCC V, which had the highest carboxylate content, relatively poor flocculation performance was exhibited in comparison with TCC IV (residual turbidity increased to 25.1 NTU). This was attributed to the size effect of TCC macromolecules. In this study, the $NaIO_4$ oxidation for ADAC was innovatively carried out under homogeneous conditions to obtain the high aldehyde content and fully oxidized cellulose samples. With excessive $NaIO_4$, the ring-opening reaction of AGUs was not dominant. The β-1,4-glycosidic bonds between AGUs began to be broken, which directly caused a decrease in the degree of polymerization of the cellulose (Liimatainen *et al*. 2012). This reduced the size of the TCC product and adversely affected its flocculation performance. Thus, TCC IV, together with its synthesis technology, is suitable for practical application in wastewater flocculation.

With the comparison to commercial CMC and APAM, the results in Fig. 7c show that the TCC IV achieved an excellent flocculation performance.

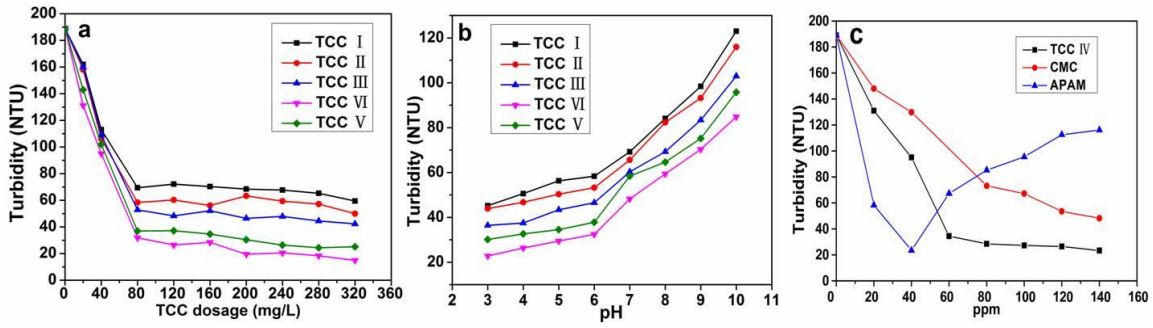

Fig. 7. Residual turbidity of the kaolin suspension (1 g/L) after coagulation-flocculation as a function of (a) flocculant TCC dosage (coagulant Al^{3+} dosage of 150 mg/L, pH of the kaolin suspension of 7, and settling time of 10 min) and (b) suspension pH (coagulant Al^{3+} and flocculant TCC dosages of 150 and 80 mg/L, respectively, settling time of 10 min); (c) comparison of flocculation performance of the TCC IV, commercial CMC and APAM.

The residual turbidity of the kaolin suspension declined to 28.5 NTU at the dosage of 60 mg/L. For reference, the cellulose-based flocculant CMC exhibited the limited flocculation performance (the residual turbidity only declined to 73.2 NTU at the dosage of 80 mg/L). After the treatment of APAM, the lowest turbidity appeared as 23.5 NTU at the dosage of 40 mg/L. But the re-stabilization phenomenon emerged with the increase of dosage. The biodegradability of APAM is also a remaining issue in comparison to natural flocculants.

Influence of pH on coagulation-flocculation

Figure 7b shows the influence of pH on the combined coagulation-flocculation with Al^{3+} and TCC. The dosages of Al^{3+} and TCC were determined from the above optimization results to be 150 and 80 mg/L, respectively. The residual turbidities of the kaolin suspensions rapidly increased after the point of pH 6. This was attributed to the coagulation property of the Al^{3+}. As shown in Fig. 6, in acidic conditions, charge neutralization and sweeping have a synergistic effect on the coagulation. This could play a facilitating role in the flocculation of the TCCs. However, in alkaline conditions, charge neutralization plays the dominant role in coagulation. The conversion from Al^{3+} to AlO^{2-} caused a negative zeta potential, which meant that part of the kaolin particles could not be coagulated by Al^{3+}. This further affected the subsequent flocculation of the TCC. Therefore, the effective pH range of the coagulant had an important influence on the process of coagulation-flocculation. The original pH 6 of the kaolin suspension was chosen for the combined coagulation-flocculation with Al^{3+} and TCC IV. Under these conditions, a residual turbidity of 28.7 NTU was finally achieved for the kaolin suspension, corresponding to a turbidity removal ratio of 95.3%.

CONCLUSIONS

1. A novel 2, 3, 6-tricarboxylate cellulose with high charge density was developed as an efficient and fully biodegradable flocculant for removal of particle contaminations from wastewater. The cellulose was innovatively carboxymethylated before $NaIO_4$ oxidation, which not only introduced carboxyl groups on the C6 of AGUs, but also allowed subsequent $NaIO_4$ oxidation under homogeneous conditions. This provided the preconditions for the final TCC products with remarkably high carboxylate contents of more than 10 mmol/g.
2. With the advantages of abundant raw materials, high charge density, and full biodegradation, the TCCs showed excellent performance in the coagulation-flocculation of kaolin suspension. A turbidity removal ratio of 95.3% was achieved for the kaolin suspension by combined coagulation-flocculation with Al^{3+} and TCC IV. The results demonstrate that these high-carboxylate content materials are good candidates for particle contamination removal in wastewater flocculation.

ACKNOWLEDGMENTS

The authors are grateful for the support of the National Natural Science Foundation of China, Grant. No. 51372226 and 61571002, the Science and Technology Program of

Zhejiang Province of China, Grant. No. 2015C32098, the Natural Science Foundation of Zhejiang Province of China, Grant. No. LY14C160004, and the Zhejiang Provincial Top Key Academic Discipline of Chemical Engineering and Technology, Grant. No. YR2011017.

REFERENCES CITED

Faris, A. H., Mohamad Ibrahim, M. N., Rahim, A. A., Hussin, M. H., and Brosse, N. (2015). "Preparation and characterization of lignin polyols from the residues of oil palm empty fruit bunch," *BioResources* 10(4), 7339-7352. DOI: 10.15376/biores.10.4.7339-7352

Faust, L., Temmink, H., Zwijnenburg, A., Kemperman, A. J. B., and Rijnaarts, H. H. M. (2014). "High loaded MBRs for organic matter recovery from sewage: Effect of solids retention time on bioflocculation and on the role of extracellular polymers," *Water Res*. 56(6), 258-266. DOI: 10.1016/j.watres.2014.03.006

Kim, U. J., and Kuga, S. (2001). "Ion-exchange chromatography by dicarboxyl cellulose gel," *J. Chromatog. A* 919(1), 29-37. DOI: 10.1016/S0021-9673(01)00800-7

Klemm, D., Heublein, B., Fink, H. P., and Bohn, A. (2005). "Cellulose: Fascinating biopolymer and sustainable raw material," *Angew. Chem. Int. Ed.* 44, 3358-3393. DOI: 10.1002/anie.200460587

Kureli, I., and Doganay, S. (2015). "The effects of surface roughness, adhesive type, and veneer species on pull-off strength of laminated medium density fibreboard," *BioResources* 10(1), 1293-1303. DOI: 10.15376/biores.10.1.1293-1303

Li, T., Zhu, Z., Wang, D. S., Yao, C. H., and Tang, H. X. (2006). "Characterization of floc size, strength and structure under various coagulation mechanisms," *Powder Technol.* 168(2), 104-110. DOI: 10.1016/j.powtec.2006.07.003

Liimatainen, H., Visanko, M., Sirviö, J. A. Hormi, O. E., and Niinimaki, J. (2012). "Enhancement of the nanofibrillation of wood cellulose through sequential periodate-chlorite oxidation," *Biomacromolecules* 13(5), 1592-1597. DOI: 10.1021/bm300319m

Liu, C. F., Sun, R. C., Qin, M. H., Zhang, A. P., Ren, J. L., Ye, J., Luo, W., and Cao, Z. N. (2008). "Succinoylation of sugarcane bagasse under ultrasound irradiation," *Bioresource Technol.* 99, 1465-1473. DOI: 10.1016/j.biortech.2007.01.062

Okita, Y., Saito, T., and Isogai, A. (2010). "Entire surface oxidation of various cellulose microfibrils by TEMPO-mediated oxidation," *Biomacromolecules* 11(6), 1696-1700. DOI: 10.1021/bm100214b

Qi, H. S., Liebert, T., Meister, F., Zhang, L., and Heinze, T. (2010). "Homogenous carboxymethylation of cellulose in the new alkaline solvent LiOH/urea aqueous solution," *Macromol. Sym.* 294(2), 125-132. DOI: 10.1002/masy.200900166

Rahul, R., Jha, U., Sen, G., and Mishra, S. (2014). "A novel polymeric flocculant based on polyacrylamide grafted inulin: Aqueous microwave assisted synthesis," *Carbohyd. Polym.* 99, 11-21. DOI: 10.1016/j.carbpol.2013.07.082

Sirviö, J., Honka, A., Liimatainen, H., Niinimäki, J., and Hormi, O. (2011). "Synthesis of highly cationic water-soluble cellulose derivative and its potential as novel biopolymeric flocculation agent," *Carbohyd. Polym.* 86(1), 266-270. DOI: 10.1016/j.carbpol.2011.04.046

Suopajärvi, T., Liimatainen, H., Hormi, O., and Niinimäki, J. (2013). "Coagulation-flocculation treatment of municipal wastewater based on anionized nanocelluloses," *Chem. Eng. J.* 231, 59-67. DOI: 10.1016/j.cej.2013.07.010

Takaichi, S., Hiraoki, R., Inamochi, T., and Isogai, A. (2014). "One-step preparation of 2, 3, 6-tricarboxy cellulose," *Carbohyd. Polym.* 110, 499-504. DOI: 10.1016/j.carbpol.2014.03.085

Takaichi, S., and Isogai, A. (2013). "Oxidation of wood cellulose using 2-azaadamantane N-oxyl (AZADO) or 1-methyl-AZADO catalyst in NaBr/NaClO system," *Cellulose* 20(4), 1979-1988. DOI: 10.1007/s10570-013-9932-4

Teotia, A. (2012). "Modification of carboxymethyl cellulose through oxidation," *Carbohyd. Polym.* 87(1), 457-460. DOI: 10.1016/j.carbpol.2011.08.005

Vandamme, D., Eyley, S., Mooter, G. V. D., Muylaert, K., and Thielemans, W. (2015). "Highly charged cellulose-based nanocrystals as flocculants for harvesting Chlorella vulgaris," *Bioresour. Technol.* 194, 270-275. DOI: 10.1016/j.biortech.2015.07.039

Wei, N., Zhang, Z. G., Liu, D., Wu, Y., Wang, J., and Wang, Q. H. (2015). "Coagulation behavior of polyaluminum chloride: Effects of pH and coagulant dosage," *Chinese J. Chem. Eng.* 23(6), 1041-1046. DOI: 10.1016/j.cjche.2015.02.003

Yang, Z., Yang, H., Jiang, Z. W., Cai, T., Li, H. B., Li, A., and Cheng, R. S. (2013a). "Flocculation of both anionic and cationic dyes in aqueous solutions by the amphoteric grafting flocculant carboxymethyl chitosan-graft-polyacrylamide," *J. Hazard. Mater.* 254-255, 36-45. DOI: 10.1016/j.jhazmat.2013.03.053

Yang, Z., Yan, H., Yang, H., Li, H. B., Li, A. M., and Cheng, R. S. (2013b). "Flocculation performance and mechanism of graphene oxide for removal of various contaminants from water," *Water Res.* 47(9), 3037-3046. DOI: 10.1016/j.watres.2013.03.027

Yang, Z., Wu, H., Yuan, B., Huang, M., Yang, H., Li, A. M., Bai, J. F., and Cheng, R. S. (2014). "Synthesis of amphoteric starch-based grafting flocculants for flocculation of both positively and negatively charged colloidal contaminants from water," *Chem. Eng. J.* 244, 209-217. DOI: 10.1016/j.cej.2014.01.083

Zhu, H. C., Zhang, Y., Yang, X. G., Liu, H. Y., Shao, L., Zhang, X. M., and Yao, J. M. (2015). "One-step green synthesis of non-hazardous dicarboxyl cellulose flocculant and its flocculation activity evaluation," *J. Hazard. Mater.* 296, 1-8. DOI: 10.1016/j.jhazmat.2015.04.029

Article submitted: February 20, 2016; Peer review completed: April 10, 2016; Revised version received and accepted: May 8, 2016; Published: May 16, 2016.
DOI: 10.15376/biores.11.3.5918-5930